

Article

# Demand-Side Management of Air-Source Heat Pump and Photovoltaic Systems for Heating Applications in the Italian Context

Elena Bee <sup>\*</sup>, Alessandro Prada  and Paolo Baggio

Department of Civil, Environmental and Mechanical Engineering, University of Trento, 38123 Trento, Italy; alessandro.prada@unitn.it (A.P.); paolo.baggio@unitn.it (P.B.)

\* Correspondence: elena.bee@unitn.it

Received: 17 October 2018; Accepted: 29 November 2018; Published: 6 December 2018



**Abstract:** Matching demand profile and solar irradiance availability is necessary to meet space heating and domestic hot water needs by means of an air-source heat pump and photovoltaic system in a single-family house. Demand-side management, with smart control of the water storage set-point, is a simple but effective technique. Several studies in the literature pursue demand-side matching and self-consumption goals through system adjustments based on the model predictive control. This study proposes a rule-based control strategy, based on instantaneous photovoltaic (PV) power production, with the purpose of enhancing the self-consumption. This strategy exploits the building's thermal capacitance as a virtual battery, and the thermal storage capacity of the system by running the heat pump to its limit when PV surplus power is available, and by eventually using an electric heater in order to reach higher temperatures. Results of annual dynamic simulations of a building and its heating system show that the proposed rule-based control strategy is able to reduce significantly the energy exchanges between the system and the grid. Despite the enlarged renewable energy share, economic analysis points out the pursuit of the self-consumption goal may lead to a diminution of the economic advantage in the Italian context (Italian weather data and the electric power pricing scheme).

**Keywords:** demand-side management; photovoltaic; air-source heat pump; self-consumption; net-metering

---

## 1. Introduction

In Europe, there is a clear long-term objective to decarbonise the energy system. The residential sector is responsible for 25.4% of the final energy consumption in the EU28 [1]; however it also represents 63% of the potential building energy savings in 2050 [2]. Currently, the average final energy demand in the EU28 residential stock is 160 kWh m<sup>-2</sup> y<sup>-1</sup> for heating, 31 kWh m<sup>-2</sup> y<sup>-1</sup> for domestic hot water, and 12 kWh m<sup>-2</sup> y<sup>-1</sup> for space cooling [3]. The share of energy consumption for space cooling is quite low, since less than 20% of the residential buildings in Europe actually meet their cooling needs, with many buildings opting to live with the discomfort of overheating rather than pay for the cost of cooling to a comfortable level [4]. An increase in the share of energy from renewable energy sources, together with more efficient energy use, are therefore required to meet the transition target toward a low-carbon society.

An air-to-water heat pump (AWHP) coupled with photovoltaic (PV) panels can play an important role in meeting the European targets, as evidenced by their increasing share in the European market. The AWHP represents the fastest growing heat pump segment across Europe, according to the European Heat Pump Market and Statistics Report 2015 [5]. The coefficient of performance (COP) of

heat pump thermodynamic cycle depends on the operating conditions (especially on the source and the sink temperatures) and on how the partial load operation is performed. For AWHPs, the large variation of the source temperature (i.e., outdoor air) significantly affects the COP, and consequently, the energy consumption. Nonetheless, inverter-driven (i.e., variable speed) compressors and other thermodynamic cycle enhancements allowed for performance improvements, both at partial and full load conditions. Therefore, the performance of the average commercial products has consistently improved in recent years [6]. Besides, the new optimized management of defrosting cycles allows the AWHP to operate even at low air temperatures, although with the drawback of a reduced COP.

However, the increased nominal and partial load efficiencies of the AWHP are not enough to ensure optimal behavior of the building and its heating, ventilation, and air conditioning (HVAC) system. For instance, some issues arise with regard to the control of the HVAC systems due to fast changes in energy demand of high performance buildings, and consequently, the building might be easily subject to poor comfort conditions [7]. Hence, an optimal design and control of the HVAC systems is essential to ensure the reduction of energy consumption and the achievement of thermal comfort for the entire heating season [8]. The challenge of minimizing energy use and cost while maintaining thermal comfort is always open. The complexity of the systems and their control strategies is increasing, since it also includes the efficient use of renewable energy sources [9]. Moreover, the AWHPs have the potential to provide flexibility to the power system, and they can reduce the grid imbalance problems due to the peaks in the PV production [10]. This is relevant in a scenario where the peaks in electricity demand are growing or where the non-dispatchable generation share is increasing [11]. Hence, the pursue of optimal self-consumption is one of the main objectives of designing the AWHP coupled with PV panels for space heating and domestic hot water preparation.

In the literature, several authors have coped with the enhancement of the self-consumption rate of locally generated power [12], and storage is becoming the key aspect [13]. The water storage tank is, to a large extent, the most common tool for reducing the discrepancy between the renewable source availability and the energy demand. Nonetheless, some authors [13,14] have demonstrated that an increase in thermal storage has very limited benefits during winter, and the self-consumption target can be achieved with standard tank sizes. Other authors [15] have found a negligible effect of storage size, except for large PV sizes or highly fluctuating electricity prices. Schibuola et al. [16] applied three control strategies to different combinations of water storage and AWHP capacities, but the results do not show any relevant variation in the energy consumption related to water storage sizes. On the contrary, large tank sizes can reduce the system efficiency unless a proper control strategy is used [17]. Prada et al. [18] studied the cost-optimal mix between the water storage tank, electrical batteries, and storage capacity of the envelope [19] in a simplified residential building in three Italian cities. The results of a multi-objective optimization process point out that about 60% of the optimal solutions have a volume lower than 150 L in Trento and Rome, and lower than 100 L in Palermo.

The necessity of a more advanced control system to maximize PV self-consumption emerges from these studies, and some attempts have been made in the literature. Psimopoulos et al. [20] used weather forecasts to take rule-based decisions on the system operation. Similarly, Thygesen and Karlsson [14] proposed a controller of the tank set point based on the radiation forecast for a ground source heat pump in the Swedish climate. However, such a controller proved to be economically unprofitable. Pospisil et al. [21] proposed a predictive control, to operate the AWHP during periods with the highest outdoor temperature. Henze et al. [22] used the time-of-use price signal to shift the electrical loads to off-peak periods at night and weekends in cooling applications. An extensive review by Péan et al. [23] clearly distinguishes between rule-based controls and model predictive controls. Almost all of the cases analyzed in the literature belong to one of these two categories. Most of these strategies, however, require advanced control systems that make them more suitable for new installations.

On the contrary, this study proposed a simple rule-based strategy that can be implemented through a low-cost controller. The simple, rule-based (i.e., if/then) control logic is based on instantaneous measurements of PV production, in order to exploit the storage tank and building

capacity with a few changes to the HVAC management system. Nevertheless, the simplicity of the rule-based control algorithm could undermine its ability to produce near-optimal control strategies. For this reason, the benefits of the proposed strategy for increasing PV self-consumption and at the same time reducing the energy drawn from the grid are analyzed. A coupled simulation of a single-family house and its energy system was set up in the TRNSYS simulation suite. Standard and TESS libraries [24] were used to model the building and the HVAC components (e.g., storage tank, PV modules, AWHP, and the control system). A TRNSYS type able to simulate variable-speed units was developed by the authors, in order to correctly model the partial load operation of the AWHP. Finally, the study focuses on the Italian context and on the analysis of the HVAC running costs. For this reason, the Italian net metering tariffs for PV systems were implemented in the simulation code.

## 2. Methods

This study proposes and tests two control strategies for demand-side management, based on instantaneous PV power production by means of dynamic simulations. A coupled simulation model of a single-family house, and the energy systems for heating (SH) and domestic hot water production (DHW), was set up by means of the TRNSYS software, using standard and TESS libraries. Annual simulations were run with a time-step of 1 min.

The Italian electricity tariffs for the year 2017 and the typical reference year for Milan (a city having a 4A climate, according to ASHRAE 90.1 classification [25]) were used as boundary conditions. Weather data included hourly profiles of dry bulb air temperature, relative humidity, global radiation, and wind speed. However, the climate can affect significantly the ASWHP performance [26].

This is an initial study focused on Northern Italy, and for this reason, does not investigate the extent to which the weather data can affect the control strategy, even if it significantly influences the PV production and the energy performance of the AWHP [26].

### 2.1. Building Model

The building is a small, bi-level, single-family house, having a volume of 275 m<sup>3</sup> and façades oriented towards the main cardinal directions. The windows are exposed to south, east, and west. The choice of this building is due to a previous modelling work of a real high-performance prototype building [26]. The walls and roof have a thermal transmittance equal to 0.25 W m<sup>-2</sup> K<sup>-1</sup>, and windows have a thermal transmittance equal to 0.9 W m<sup>-2</sup> K<sup>-1</sup>. The ventilation rate of the building is 0.5 ACH (air change per hour), according to Italian technical specification UNI/TS 11300-1 [27], and ventilation is performed by a mechanical ventilation system with a heat recovery exchanger. The building is representative of a European family house, since the floor area (about 80 m<sup>2</sup>) is quite close to the average European floor area of a residential dwelling (i.e., 84 m<sup>2</sup>) [28]. The building modeled is divided into four thermal zones, three of which are equipped with radiant floor panels. A small mechanical room is without a heating terminal, but has internal heat gains due to the tank thermal losses. A weekly pattern represents the total internal gain due to people and appliances, with two different profiles for the living room/kitchen and for the bedrooms. The profiles are taken from the Italian technical specification UNI TS 11300-1 [27]. The building model and the input/output management is performed by means of Type 56 (standard TRNSYS library).

### 2.2. Heating, Ventilation, and Air Conditioning System and the Domestic Hot Water Production Model

The heating system was based on a variable-speed AWHP, coupled with radiant floor panels (Figure 1). The AWHP simulation model was based on the performance map and on the partial-load performance function provided by the manufacturer. A high-performance unit with a COP value of 4.5 at 7–35 °C and a nominal heating capacity of 5 kW is considered in this study. As usual with high-performance units, the partial-load operation performance curve is such that the optimal AWHP performance happens when it is operating at around 50% of the load, and the maximum COP is up to 30% higher than the COP at the nominal capacity. The compressor speed depends on the control

strategy, and it takes different variables as input. In the reference case, for the SH mode the speed linearly depended on the distance of the temperature from the set-point in the SH tank, while for the DHW mode the AWHP was always run at the maximum speed. Cross-linked polyethylene (PEX) pipes were used for the radiant panels, with a diameter of 0.016 m, pipe spacing of 0.12, and thermal conductivity of  $0.44 \text{ W m}^{-1} \text{ K}^{-1}$ . An on-off temperature controller in each room controlled the ambient temperature, with a dead-band of  $\pm 0.5 \text{ }^\circ\text{C}$ . Two separate water storage tanks were used for SH and DHW, and a temperature controller (with dead-band of  $3 \text{ }^\circ\text{C}$  around the set-point) controls their temperatures. The set-point temperature of the SH tank is reset based on the outdoor temperature, and it varies linearly between  $38 \text{ }^\circ\text{C}$  and  $28 \text{ }^\circ\text{C}$  as the outdoor air temperature varies between  $-5 \text{ }^\circ\text{C}$  and  $15 \text{ }^\circ\text{C}$ . The set-point temperature of the DHW tank was set to  $45 \text{ }^\circ\text{C}$  in the reference case. The water storage tanks were modeled as stratified vertical cylindrical tanks, with a volume of 150 L for space heating and 250 L for DHW production. Priority is given to DHW demand, which is modeled through the M standard tapping profile according to the EN 16147 [29]. A mechanical ventilation system with heat recovery (with a nominal efficiency of 75%) guarantees a ventilation rate of 0.5 ACH in each room. A typical commercial PV module was used in the simulation (Table 1). Since the PV production greatly affects the control efficiency, the PV area is a parametric value in this study. Hence, three different PV areas are considered, i.e.,  $15 \text{ m}^2$  (PV15),  $20 \text{ m}^2$  (PV20), or  $30 \text{ m}^2$  (PV30), corresponding, respectively, to the peak powers of 2.1 kW, 2.8 kW, and 4.2 kW. The PV electric power production, when available, is used by the AWHP, and if necessary, additional electric power is taken from the grid. PV surplus power is delivered to the grid, and the model assumes a conversion efficiency (DC/AC inverter) of 90%.

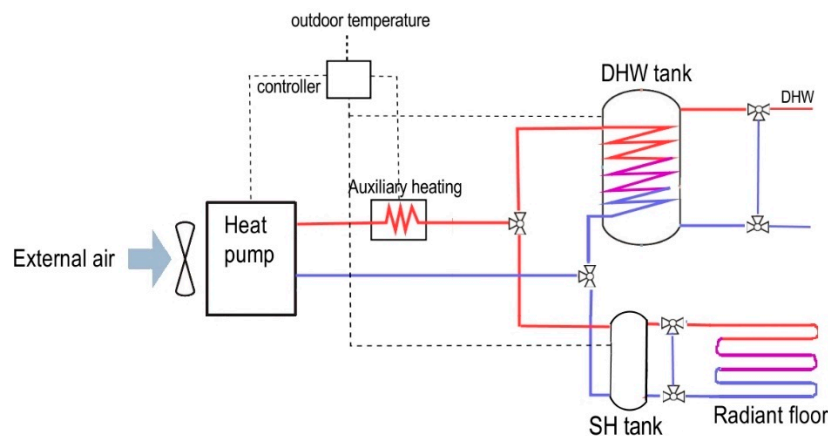


Figure 1. Heating system layout.

Table 1. Technical specifics of the photovoltaic (PV) modules.

Module Specifics	Value	Units
Area	1.6	$\text{m}^2$
Power Rating at Standard Test Conditions	230	W
Efficiency	14.1%	-
Number of cells	60	-
Maximum power point current	7.8	A
Maximum power point voltage	29.5	V
Short circuit current	8.4	A
Open circuit voltage	37	V
Tilt angle	10	deg

### 2.3. Economics

The electricity market is set up to match energy supply and demand in Italy. For this reason, there is trading between generators and suppliers in the Italian Power Exchange. The increasingly

widespread diffuse electricity production and the growing number of heat pump installations are altering the grid balance and in order to face those changes, the electricity market is evolving. Italian energy providers have recently introduced a time-of-use tariff for the domestic users that does not penalize consumers with large annual electricity needs. This rate will promote the adoption of AWHPs for space heating or cooling. The time-of-use tariff has two electricity prices that change every three months (Figure 2a). During the weekdays, the F1 price is used from 8:00 AM to 7:00 PM, while the F23 price is available from 7:00 PM to 8:00 AM. The F23 is also applied for the weekends. The annual electricity bill also includes fixed costs (about 159 €/y for a committed power of 4.5 kW) and 13% of fees (in 2017) [30]. The daily profiles of the time-of-use tariff, including transport/management and system charges, are shown in details in Figure 2a. Figure 2b represents instead a typical profile of the real price on the market (unique national price; PUN) that reflects the unbalance of electricity exchanges between the grid and the consumers/producers.

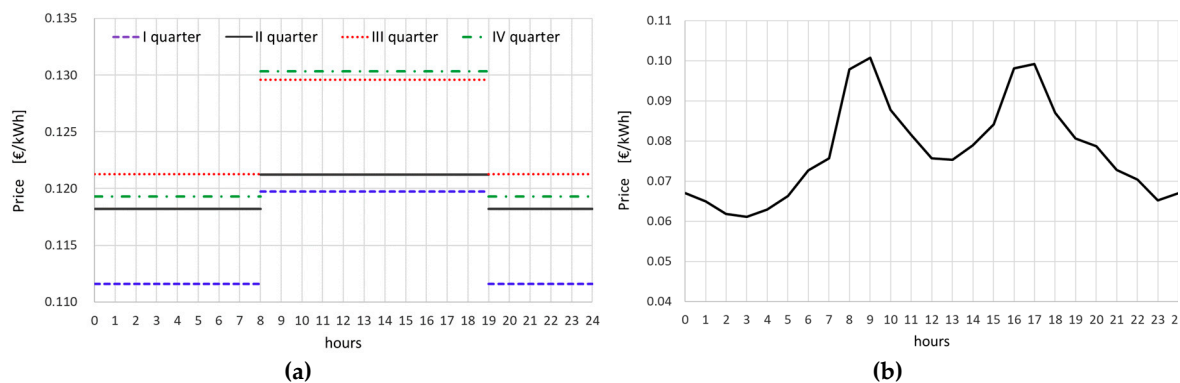


**Figure 2.** (a) Italian electricity time-of-use tariffs for domestic users in 2017. Prices include transport/management and system charges and annual fixed costs, but fees are not included. (b) Unique national price (PUN) on a weekday for the year 2017 with the typical double-peak profile.

A separate national net-metering scheme rewards and incentivizes power production from renewable energy sources. In the Italian net-metering scheme, the power generated by eligible on-site renewable plants can be delivered to the grid and used to offset the electricity withdrawn from the grid. The grid authority pays a contribution based on the balance and the economic value of power injections and withdrawals in a given calendar year. The contribution amount, calculated with Equation (2), is based on the energy exchanges with the grid ( $E_{grid}$ ,  $E_{grid}$ ) and some economic indices of the national market, such as the day ahead of auction market (MGP), the unique national price (PUN), and the price of the flat-rate exchange ( $CU_{sf}$ ) [31,32].

The annual economic balance is defined in Equation (1), where *Bill* is the cost of purchased electricity, *C<sub>s</sub>* and *Exc* are the contributions, defined respectively with Equations (2) and (3), and the *Netbill* is the amount actually paid at the end of the year by the householder. The economic credit (*Exc*) is granted only if the economic value of the electricity fed to the grid is higher than the economic value of the withdrawn power, according to Equation (3).

$$Net\ bill = Bill - C_s - Exc \tag{1}$$

$$C_s = \min(E_{from\ grid} \cdot PUN; E_{to\ grid} \cdot MGP) + CU_{sf} \cdot \min(E_{from\ grid}, E_{to\ grid}) \tag{2}$$

$$Exc = \max(0; E_{to\ grid} \cdot MGP - E_{from\ grid} \cdot PUN) \tag{3}$$

#### 2.4. Control System Strategy

The proposed control strategy aims to increase self-consumption by changing the set-point temperatures as a function of the actual PV generation. In a previous work [30], different algorithms,

based on either the PV production or the outdoor temperature, were compared to each other. The authors found that the temperature has a limited impact on the control reliability with respect to the control, based on the PV production. In the previous study, the algorithm checks whether PV power is still available after standard set-points are met. If this is the case, the algorithm increases the set-points of the DHW tank, the SH tank, and ambient thermostats and, consequently, it runs the AWHP to satisfy the new set-points. In addition, the set-points are slightly reduced in case of low or absent PV power.

In this study, we propose a new control strategy (HP+) as a further development of the algorithm, based on PV production [33]. The new algorithm first checks the AWHP capacity, and in this respect, the available PV power is compared with the minimum and the maximum power absorption of the AWHP. The increase in set-points is therefore calculated as a function of this difference. The maximum set-point variation is applied in the case when PV production is greater than the power absorption at the maximum AWHP speed. Otherwise, only a fraction of the maximum set-point variation is applied. The set-points are only increased and not reduced, with the purpose of avoiding any possible discomfort (even if acceptable). Besides, the algorithm comparability with the reference case is ensured since the same indoor conditions are pursued. The maximum set-points are 55 °C for the water tanks (the maximum temperature supply of the AWHP) and 22 °C for the air ambient temperature. Moreover, another rule-based control scheme is implemented. This new function checks whether PV power is still available after the maximum set-point temperature is reached in the tanks. In this case, the excess power is used to heat the DHW storage to a higher temperature (up to 90 °C for safety reasons) by means of an electric heater (two subsequent stages of 500 W). This strategy maximizes the self-consumption of PV production, although with the drawback of a high exergetic cost of the electric resistance, which affects the overall efficiency of the system. The function is called electric heater plus (EH+). The two functions are applied either independently or in combination (HP+ and EH+), but with HP+ priority.

$$T_{set,HP+} = T_{set,ref} + \frac{T_{set,max} - T_{set,ref}}{P_{abs,max} - P_{abs,min}} \cdot \max(0; P_{PV,surplus} - P_{abs,min}) \quad (4)$$

$$T_{set,EH+} = T_{max,DHW} \cdot \max(0; P_{PV,surplus} - P_{abs,max}) \cdot \max(0; T_{tank} - T_{set,ref}) \quad (5)$$

Notice that a temperature-controlled mixing valve is installed, both on the DHW and the SH supply system. This secondary control, connected to a three-way valve, mixes the water exiting from the tanks with cold water in order to meet the supply water temperature (i.e., 45 °C for DHW and depending on the outdoor reset control for the SH).

The different level of self-consumption is quantified by two indices. These two key figures are the self-consumption ratio ( $SC_{ratio}$ ) and the self-sufficiency ratio ( $SS_{ratio}$ ), which are detailed in Equations (6) and (7), respectively.

$$SC_{ratio} = \frac{Selfconsumption[kWh]}{PVproduction[kWh]} \quad (6)$$

$$SS_{ratio} = \frac{Selfconsumption[kWh]}{Totalconsumption[kWh]} \quad (7)$$

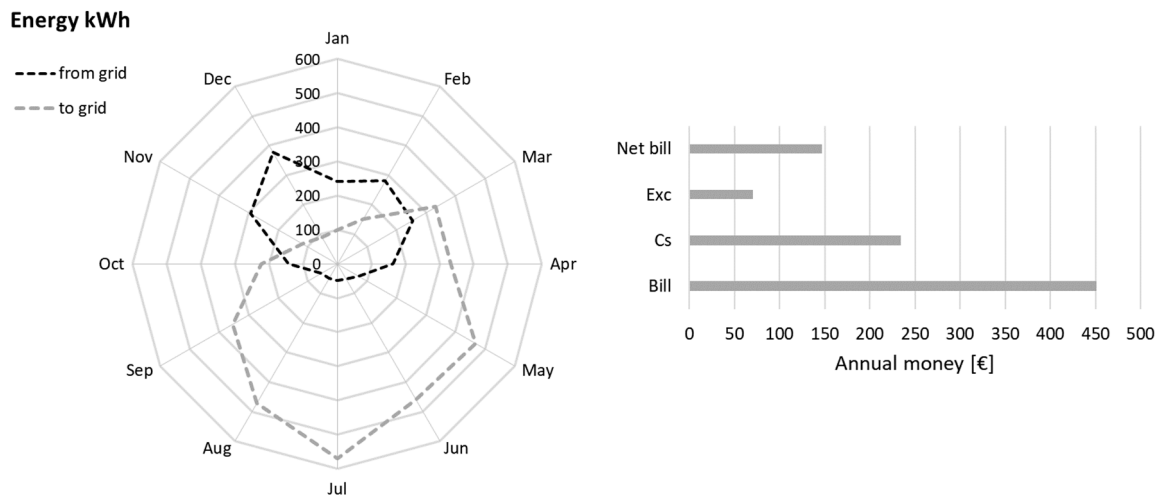
The two indices quantify the optimality of the control in a different way. The self-consumption ratio evaluates the portion of energy produced by the PV that is directly consumed, while the self-sufficient ratio quantifies the share of total energy consumption for SH and DHW produced by using the PV source.

### 3. Results

The results are presented as a comparison between the reference case, in which the system is controlled using the standard approach, and the cases in which the new control strategies (Section 2.4) are applied.

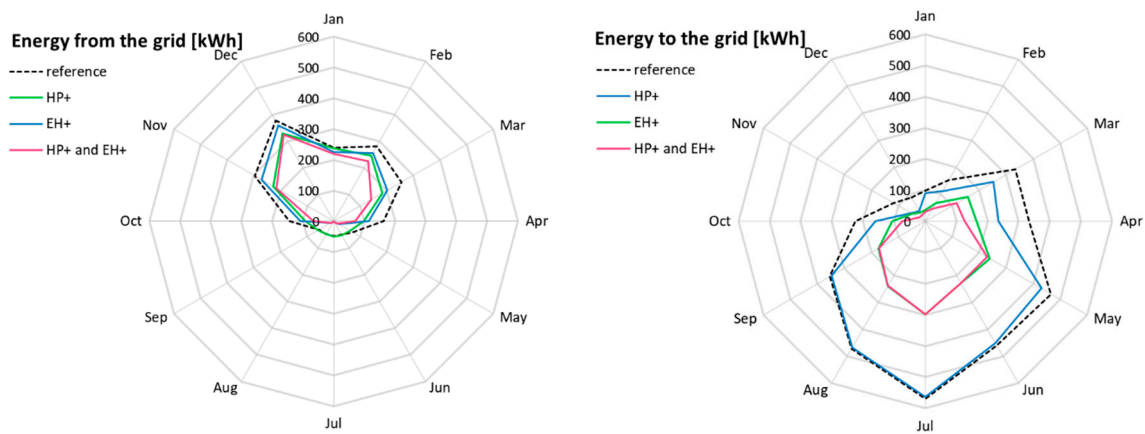
Energy use, self-consumption (direct use of the energy generated by PV panels), and energy exchanged with the grid, are presented on a monthly or annual basis. Bills and contributions are evaluated on an annual basis.

In the reference case, the annual  $SC_{ratio}$  is 7%, and the remaining energy from the PV system is delivered to the grid. Such a low value is due to the configuration of the model, where no cooling applications or domestic appliances are taken into account, as explained in the introduction. Only the DHW needs are covered in the summer months, and consequently, a large amount of surplus energy is produced. Figure 3 includes some significant results about the simulation of the reference case. On the left, the monthly energy exchanged with the grid is represented, and it is evident that the energy to the grid exceeds the energy from the grid, especially in summer. On the right, annual costs/incomes for the householder on the base of the net-metering scheme indicate that the contribution considerably reduces the *Netbill*.



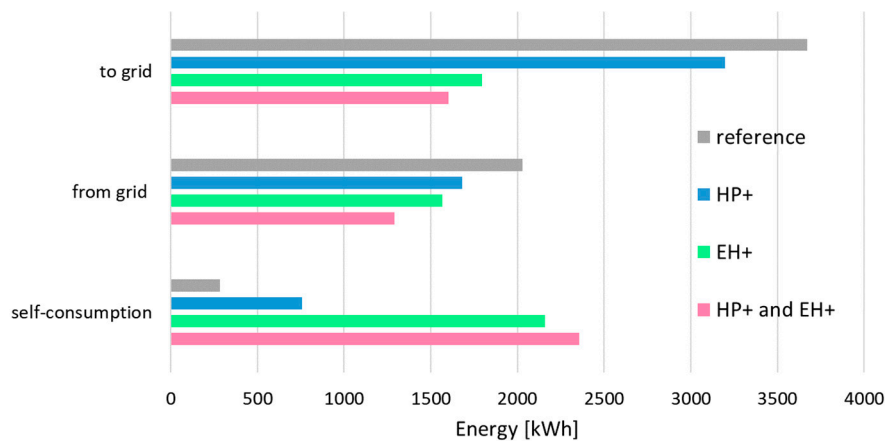
**Figure 3.** Reference case: monthly energy exchanges with the grid and annual bills/takings for the householder with net-metering (Equations (1)–(3)).

Figure 4 compares the three simulations with the new control strategies to each other and to the reference case, in terms of monthly energy fluxes. All of the algorithms applied have the effect of reducing the exchanges with the grid (energy drawn from the grid and energy delivered to the grid). In other words, the algorithms improve the self-consumption and the self-sufficiency, especially when the HP+ and EH+ are combined together. In this case, the  $SC_{ratio}$  increases from 7% to 60%, and the  $SS_{ratio}$  from 12% to 65%. This result therefore highlights the potential benefit for the grid manager if this algorithm were extensively applied in buildings with PV systems.



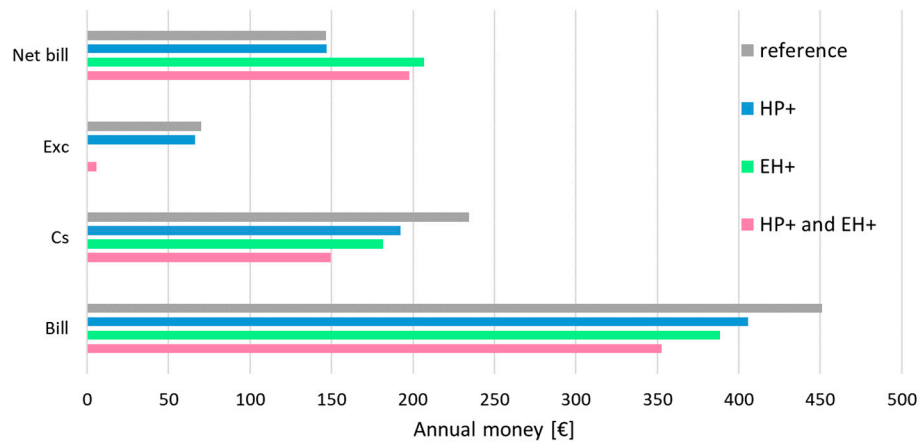
**Figure 4.** Monthly energy exchanges with the grid for the reference case, and for the cases with the new control algorithms (PV area of 20 m<sup>2</sup>).

The reduction of the energy exchanges is also evident from Figure 5, in which the increase of self-consumption is also shown on the annual balance. This increase is quantified as 167% for HP+, 660% for EH+, and 729% for HP+ and EH+, with respect to the reference case. Note that the self-consumption exceeds the energy drawn from the grid when the EH+ or the HP+ combined with EH+ algorithms are adopted.



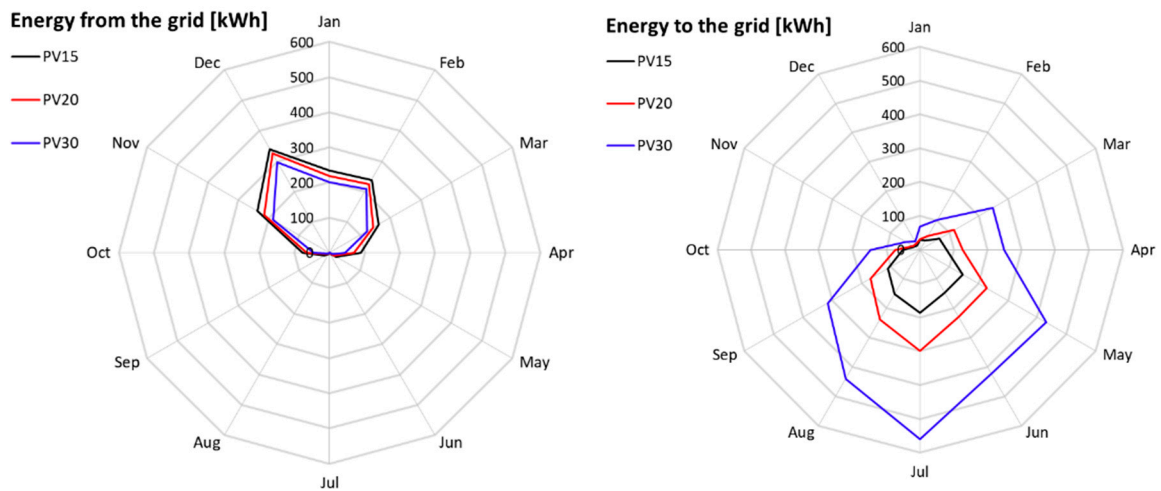
**Figure 5.** Annual amounts of energy exchanged with grid and self-consumed for the reference case and for the cases with the new control strategies (PV area of 20 m<sup>2</sup>).

Figure 6 compares the three simulations with the new control strategies to one another and to the reference case, in economic terms. The new algorithms are not advantageous in economic terms, although the energy taken from the network is greatly reduced. The resulting *Netbill* increases because the contribution ( $C_s$ ) decreases for higher self-consumption levels. That means that these control strategies aimed at increasing the self-consumption are not favored by the Italian net-metering scheme, which does not adequately reward such behavior.



**Figure 6.** Annual bills/takings for the householder on the base of the net-metering scheme (Equations (1)–(3)) for the reference case and the cases with control strategies applied (PV area of 20 m<sup>2</sup>).

Finally, Figures 7 and 8 show the influence of the PV array area (or aperture) on the energy exchanges and costs. Figure 7 clearly shows how, passing from 15 m<sup>2</sup> to 30 m<sup>2</sup>, the energy withdrawn from the grid obviously decreases, and the energy fed into the grid increases. With a PV area of 15 m<sup>2</sup>, the energy withdrawn exceeds the energy delivered to the grid. The  $SS_{ratio}$  increases from 65% (PV15) to 58% (PV20) and 72% (PV30) by oversizing the area, while the  $SC_{ratio}$  increases from 60% (PV15) to 65% (PV20), but then decreases to 48% (PV30).



**Figure 7.** Monthly energy exchanges with the grid for the case with control strategy HP+ and EH+, and for a PV area of 15, 20, and 30 m<sup>2</sup>.

Figure 8 shows the different effects of the contribution to the *Netbill* from an economic point of view. In both the case with HP+ only and with HP+ and EH+, the  $Exc$  term is equal to zero, and the  $C_s$  term is lower for the smaller area size; the resulting *Netbill* penalizes this situation. Therefore, an oversized system is more profitable, compared to one that is more suitable to the actual energy needs of the building by considering the running costs. Nonetheless, the different installation costs and the payback times should also be considered.

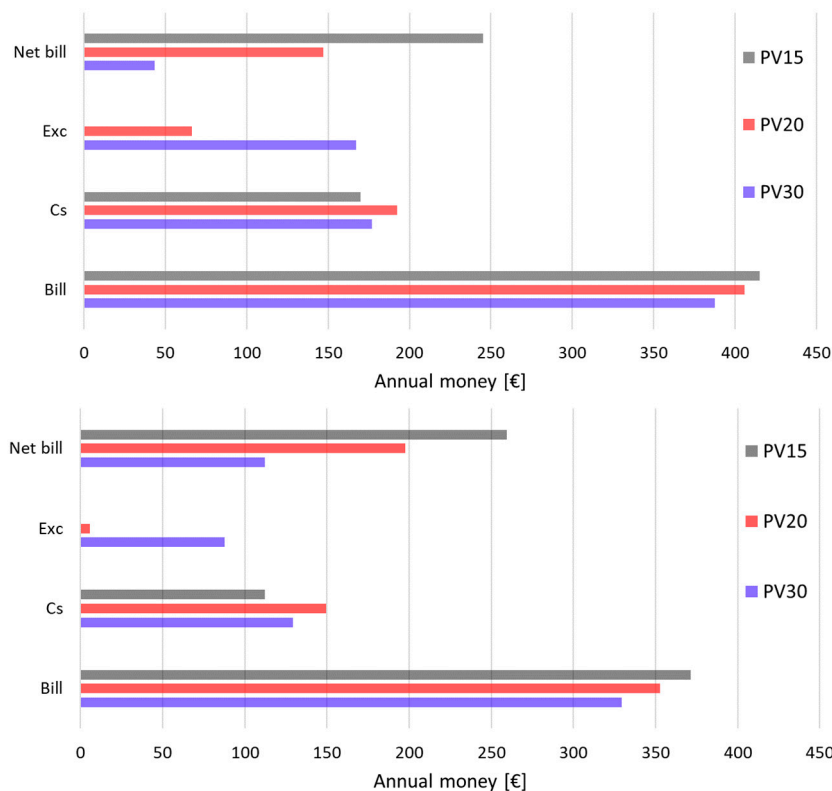


**Figure 8.** Annual bills/takings for the householder on the base of the net-metering scheme (Equations (1)–(3)) for the case with control strategy HP+ only (**above**) and HP+ EH+ (**below**), as well as for a PV area of 15, 20, and 30 m<sup>2</sup>.

#### 4. Conclusions

Householders who take part in the Italian net-metering scheme receive a contribution that significantly reduces their net annual spending for electricity. The contribution boosts the installation of PV plants, helping to meet the goal of the progressive de-carbonization of the dwelling sector.

The regular bill (time-of-use tariff) linearly depends on the purchased electricity, and decreases when a control strategy oriented to self-consumption is applied. Despite the benefits of those control strategies, in terms of self-consumption and energy exchanges, the Italian net-metering contribution does not boost the optimal use of the self-produced electricity in terms of net cost, resulting in larger net money savings for management of the system with larger energy exchanges with the national grid. In particular, if the HP+ and EH+ strategies are applied together, the energy delivered to the grid and drawn from the grid decrease by 56% and 36%, respectively, but the net bill increases by 34%.

A threshold for the PV array area, below which the energy withdrawn exceeds the energy delivered to the grid, can be identified for a particular system configuration and energy use. The economic advantages are obviously lower for smaller areas, although more suitable for the building energy demand. It worth noting, however, that a correct sizing procedure would require taking into account other electrical uses that are not included in this study, and a comprehensive economic analysis should include the initial investment, maintenance, and replacement costs of the PV system.

**Author Contributions:** E.B. and A.P. defined the methods, ran simulation and analyzed the results. P.B. identified the aims of the research and supervised the study. All authors contributed in writing, editing, and structuring the paper.

**Acknowledgments:** The authors want to thank INNOVA Renewing Energies for the fruitful collaboration in analyzing the heat pump operation.

**Conflicts of Interest:** The authors declare no conflict of interest.

## References

1. Eurostat. Complete Energy Balances—Annual Data 2016. Available online: <https://ec.europa.eu/eurostat/statistics-explained/index.php> (accessed on 1 October 2018).
2. IEA. *Energy Technology Perspectives 2010—Scenarios & Strategies to 2050*; IEA: Paris, France, 2010.
3. HotMaps. *Hotmaps Report D2.3 WP2 Open Dataset for the EU28*; HotMaps: Vienna, Austria, 2018. [CrossRef]
4. Stratego. Low Carbon Heating and Cooling Strategies for Europe. Final Report of the EU Project “Stratego Enhanced Heating & Cooling Plans”. Available online: <http://stratego-project.eu/reports/> (accessed on 1 October 2018).
5. Nowak, T.; Westring, P. *European Heat Pump Market and Statistics Report 2016*; Technical report; The European Heat Pump Association AISBL (EHPA): Brussels, Belgium, 2016.
6. Chua, K.J.; Chou, S.K.; Yang, W.M. Advances in heat pump systems: A review. *Appl. Energy* **2010**, *87*, 3611–3624. [CrossRef]
7. Penna, P.; Prada, A.; Cappelletti, F.; Gasparella, A. Multi-objectives optimization of energy efficiency measures in existing buildings. *Energy Build.* **2015**, *95*, 57–69. [CrossRef]
8. Carlon, E.; Schwarz, M.; Prada, A.; Golicza, L.; Verma, V.K.; Baratieri, M.; Gasparella, A.; Haslinger, W.; Schmidl, C. On-site monitoring and dynamic simulation of a low energy house heated by a pellet boiler. *Energy Build.* **2016**, *116*, 296–306. [CrossRef]
9. Fabrizio, E.; Seguro, F.; Filippi, M. Integrated HVAC and DHW production systems for Zero Energy Buildings. *Renew. Sustain. Energy Rev.* **2014**, *40*, 515–541. [CrossRef]
10. Fischer, D.; Madani, H. On heat pumps in smart grids: A review. *Renew. Sustain. Energy Rev.* **2017**, *70*, 342–357. [CrossRef]
11. Arteconi, A.; Hewitt, N.J.; Polonara, F. State of the art of thermal storage for demand-side management. *Appl. Energy* **2012**, *93*, 371–389. [CrossRef]
12. Luthander, R.; Widén, J.; Nilsson, D.; Palm, J. Photovoltaic self-consumption in buildings: A review. *Appl. Energy* **2015**, *142*, 80–94. [CrossRef]
13. Fischer, D.; Rautenberg, F.; Wirtz, T.; Wille-Haussmann, B.; Madani, H. Smart meter enabled control for variable speed heat pumps to increase PV self-consumption. In Proceedings of the 24th IIR, Yokohama, Japan, 16–22 August 2015.
14. Thygesen, R.; Karlsson, B. Simulation of a proposed novel weather forecast control for ground source heat pumps as a mean to evaluate the feasibility of forecast controls’ influence on the photovoltaic electricity self-consumption. *Appl. Energy* **2016**, *164*, 579–589. [CrossRef]
15. Arteconi, A.; Hewitt, N.J.; Polonara, F. Domestic demand-side management (DSM): Role of heat pumps and thermal energy storage (TES) systems. *Appl. Therm. Eng.* **2013**, *51*, 155–165. [CrossRef]
16. Schibuola, L.; Scarpa, M.; Tambani, C. Demand response management by means of heat pumps controlled via real time pricing. *Energy Build.* **2015**, *90*, 15–28. [CrossRef]
17. De Coninck, R.; Baetens, R.; Verbruggen, B.; Driesen, J.; Saelens, D.; Helsens, L. Modelling and simulation of a grid connected photovoltaic heat pump system with thermal energy storage using Modelica. In Proceedings of the 8th International Conference on System Simulation, Paris, France, 8–10 November 2010.
18. Prada, A.; Bee, E.; Grigante, M.; Baggio, P. On the optimal mix between lead-acid battery and thermal storage tank for PV and heat pump systems in high performance buildings. *Energy Procedia* **2017**, *140*, 423–433. [CrossRef]
19. Kats, G.; Seal, A. Buildings as Batteries: The Rise of ‘Virtual Storage’. *Electr. J.* **2012**, *25*, 59–70. [CrossRef]
20. Psimopoulos, E.; Bee, E.; Luthander, R.; Bales, C. Smart control strategy for PV and heat pump system utilizing thermal and electrical storage and forecast services. In Proceedings of the Solar World Congress 2017, Abu Dhabi, UAE, 29 October–2 November 2017.
21. Pospíšil, J.; Spilacek, M.; Kudela, L. Potential of predictive control for improvement of seasonal coefficient of performance of air source heat pump in Central European Climate Zone. *Energy* **2018**, *154*, 415–423. [CrossRef]
22. Henze, G.P.; Felsmann, C.; Knabe, G. Evaluation of optimal control for active and passive building thermal storage. *Int. J. Therm. Sci.* **2004**, *43*, 173–183. [CrossRef]
23. Péan, T.Q.; Saloma, J.; Costa-Castelló, R. Review of control strategies for improving the energy flexibility provided by heat pump systems in buildings. *J. Process Control* **2018**, in press.

24. TESS Component Libraries. Available online: <http://www.trnsys.com/tess-libraries/> (accessed on 10 September 2018).
25. ASHRAE. *International Weather for Energy Calculations (IWEC Weather Files)*; ASHRAE: Atlanta, GA, USA, 2001.
26. Bee, E.; Prada, A.; Baggio, P. Air-source heat pump and photovoltaic systems for residential heating and cooling: Potential of self-consumption in different European climates. *Build. Simul. Int. J.* **2019**, in press.
27. UNI. *UNI/TS 11300. Prestazioni energetiche degli edifici—Parte 1: Determinazione del fabbisogno di energia termica dell'edificio per la climatizzazione estiva ed invernale*; Ente Nazionale Italiano di Normazione: Milano, Italy, 2016.
28. ENTRA NZE Project, Co-Founded by Intelligent Energy Europe Programme. Available online: [www.entranze.enerdata.eu](http://www.entranze.enerdata.eu) (accessed on 1 October 2018).
29. CEN. *EN 16147:2017 Heat Pumps with Electrically Driven Compressors—Testing, Performance Rating and Requirements for Marking of Domestic Hot Water Units*; European Committee for Standardization: Brussels, Belgium, 2017.
30. ARERA. Available online: [www.arera.it/it/prezzi.htm](http://www.arera.it/it/prezzi.htm) (accessed on 1 October 2018).
31. ARERA. Available online: [www.arera.it/it/comunicati/18/180403.htm](http://www.arera.it/it/comunicati/18/180403.htm) (accessed on 1 October 2018).
32. GSE. Servizio di Scambio sul Posto Disposizioni Tecniche di Funzionamento. 2016. Available online: [www.gse.it/servizi-per-te/fotovoltaico/scambio-sul-posto/documenti](http://www.gse.it/servizi-per-te/fotovoltaico/scambio-sul-posto/documenti) (accessed on 1 October 2018).
33. Bee, E.; Prada, A.; Baggio, P. Rule Based Control Strategies of Thermal Storage in Residential Heating Systems with Air-Source Heat Pump and Photovoltaic Panels. In Proceedings of the 5th International High Performance Buildings Conference, West Lafayette, IN, USA, 9–12 July 2018.



© 2018 by the authors. Licensee MDPI, Basel, Switzerland. This article is an open access article distributed under the terms and conditions of the Creative Commons Attribution (CC BY) license (<http://creativecommons.org/licenses/by/4.0/>).